Artif Life Robotics (2008) 13:377–381
DOI 10.1007/s10015-008-0585-6

ORIGINAL ARTICLE

Takashi Yatoh · Shinichi Sagara · Masakazu Tamura

Digital type disturbance compensation control of a floating underwater robot with 2 link manipulator

Received and accepted: August 5, 2008

Abstract We have proposed continuous and discrete time resolved acceleration control methods for underwater vehicle-manipulator systems and the effectiveness of the control methods have been shown by experiments. In this paper, we propose a digital type disturbance compensation control method based on the RAC method considering singular configuration of manipulator. Experimental results show the effectiveness of the proposed method.

Key words Underwater robot · Manipulator · Digital control · Observer

List of symbols

Σ_U: inertial coordinate frame
Σ_i: link i coordinate frame (i = 0, 1, 2; link 0 means base)
${}^U\boldsymbol{R}_i$: coordinate transformation matrix from Σ_i to Σ_U
$\boldsymbol{p}_e$: position vector of end-tip of manipulator with respect to Σ_U
$\boldsymbol{p}_0$: position vector of origin of Σ_0 with respect to Σ_U
$\boldsymbol{v}_i$: linear velocity vector of Σ_i with respect to Σ_U
$\boldsymbol{\omega}_i$: angular velocity vector of Σ_i with respect to Σ_U
$\boldsymbol{\phi}_i$: relative angle of joint i
$\boldsymbol{x}_0$: position and attitude vector of Σ_0 with respect to Σ_U ($= [\boldsymbol{p}_0^T \quad \phi_0]^T$)
$\boldsymbol{\phi}$: relative joint angle vector ($= [\phi_1 \ \phi_2]^T$)
m_i: mass of link i
l_i: length of link i
V_i: volume of link i
D_i: width of link i
C_{D_i}: drag coefficient of link i
ρ: fluid density
$\boldsymbol{a}_i$: position vector from joint i to center of gravity of link i with respect to Σ_U
$\boldsymbol{b}_i$: position vector from joint i to center of buoyancy of link i with respect to Σ_U
$\boldsymbol{E}$: identity matrix
$\boldsymbol{g}$: gravitational acceleration vector
F_j: thruster force (j = 1, 2, 3)
R: length form origin of Σ_0 to thruster

T. Yatoh · S. Sagara (✉) · M. Tamura
Department of Control Engineering, Kyushu Institute of Technology, Tobata, Kitakyushu 804-8550, Japan
e-mail: sagara@cntl.kyutech.ac.jp

This work was presented in part at the 12th International Symposium on Artificial Life and Robotics, Oita, Japan, January 25–27, 2007

1 Introduction

Underwater Vehicle-Manipulator Systems (UVMSs) are expected to make important roles in ocean exploration. Many studies about dynamics and control of UVMS have been reported,[1–8] however the experimental studies are only a few.

We have proposed analog and digital Resolved Acceleration Control (RAC) methods for UVMS,[9–11] and the effectiveness of the RAC methods are demonstrated by using a floating underwater robot with vertical planar 2-link manipulator shown in Fig. 1. Furthermore, we have proposed a RAC method considering singular configuration of manipulator.[12]

In general, added mass, added moment of inertia and drag coefficient are used constant value that depends on the shape of the robots.[13] Our proposed methods described above can reduce the influence of hydrodynamic force by position and velocity feedbacks.

In this paper, to obtain higher control performance we propose a digital type disturbance compensation control method based on the RAC method considering singular configuration of manipulator.[12] The influence of hydrodynamic force is treated as a disturbance, and the disturbance is compensated by using a disturbance observer.

To verify the effectiveness of the RAC method with the disturbance observer, experiments using the 2-link underwater robot are performed. The experimental results show that the control method has a good control performance.

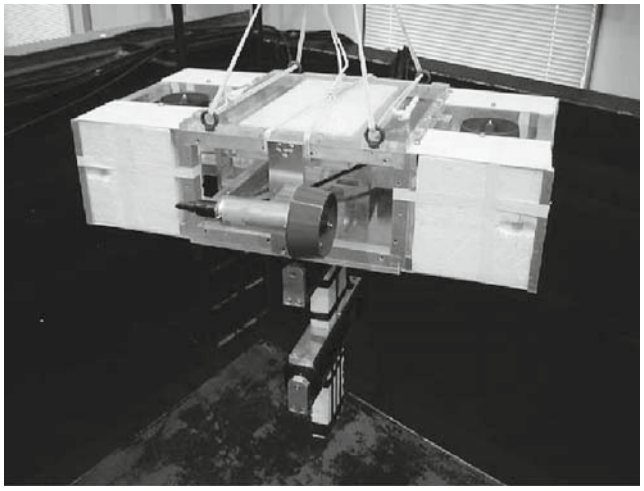

Fig. 1. Floating 2-link underwater robot

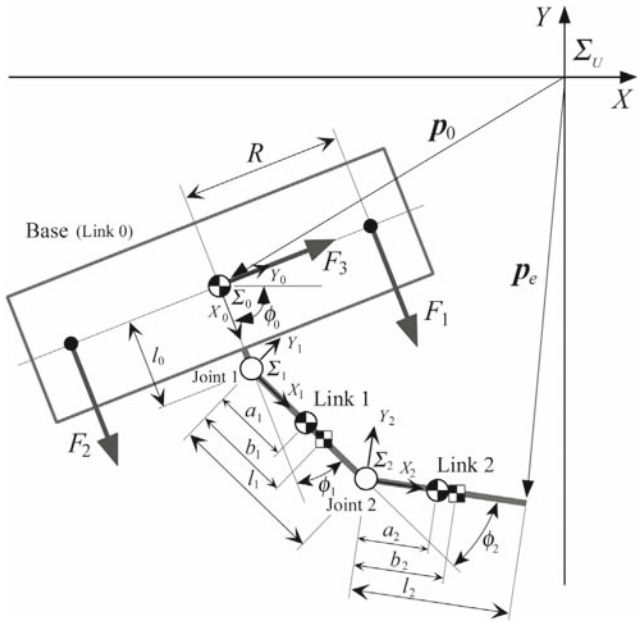

Fig. 2. 2-link underwater robot model

2 Modeling

The underwater robot model used in this paper is shown in Fig. 2. It has a robot base and a 2-DOF manipulator which can move in a vertical plane. Thrusters are mounted on the base to provide propulsion for position and attitude control of the base.

From Fig. 2 kinematic and momentum equations can be obtained[9]:

$$\dot{\boldsymbol{p}}_e = \boldsymbol{A}\dot{\boldsymbol{x}}_0 + \boldsymbol{B}\dot{\boldsymbol{\phi}}, \quad \dot{\boldsymbol{s}} = \boldsymbol{C}\dot{\boldsymbol{x}}_0 + \boldsymbol{D}\dot{\boldsymbol{\phi}} \tag{1}$$

where $\boldsymbol{A} \in \boldsymbol{R}^{2\times3}$ and $\boldsymbol{B} \in \boldsymbol{R}^{2\times2}$ are matrices consisting of attitude angle of base and joint angles. $\boldsymbol{C} \in \boldsymbol{R}^{3\times3}$ and $\boldsymbol{D} \in \boldsymbol{R}^{3\times2}$ are matrices including the mass, added mass, inertia and added inertia of the base and links.

In the meanwhile, the drag force and moment of joint i can be generally represented as follows[14]:

$$\boldsymbol{f}_{d_i} = \frac{\rho}{2} C_{D_i} D_i^U \boldsymbol{R}_i \int_0^{l_i} \|\boldsymbol{w}_i\| \boldsymbol{w}_i dx_i \tag{2}$$

$$\boldsymbol{t}_{d_i} = \frac{\rho}{2} C_{D_i} D_i^U \boldsymbol{R}_i \int_0^{l_i} \hat{\boldsymbol{x}}_i \times \|\boldsymbol{w}_i\| \boldsymbol{w}_i dx_i \tag{3}$$

where

$$\boldsymbol{w}_i = \begin{bmatrix} 0 & 0 & 0 \\ 0 & 1 & 0 \\ 0 & 0 & 1 \end{bmatrix} {}^i\boldsymbol{R}_U (\boldsymbol{v}_i + \boldsymbol{\omega}_i \times \hat{\boldsymbol{x}}_i), \quad \hat{\boldsymbol{x}}_i = [x_i \quad 0 \quad 0]^T$$

Furthermore, the gravitational and buoyant forces acting on link i are described as

$$\boldsymbol{f}_{g_i} = (\rho V_i - m_i)\boldsymbol{g} \tag{4}$$

$$\boldsymbol{t}_{g_i} = (\rho V_i \boldsymbol{b}_i - m_i \boldsymbol{a}_i) \times \boldsymbol{g} \tag{5}$$

Considering the hydrodynamic forces described above and using Newton-Euler formulation, the following equation of motion can be obtained:

$$\boldsymbol{M}(\boldsymbol{q})\ddot{\boldsymbol{q}} + \boldsymbol{N}(\boldsymbol{q}, \dot{\boldsymbol{q}})\dot{\boldsymbol{q}} + \boldsymbol{f}_D = [f_x \quad f_y \quad \tau_0 \quad \tau_1 \quad \tau_2]^T \tag{6}$$

where $\boldsymbol{q} = [\boldsymbol{x}_0^T \ \boldsymbol{\phi}^T]^T$ and $\boldsymbol{M}(\boldsymbol{q})$ is the inertia matrix consisting of the added mass and inertia, $\boldsymbol{N}(\boldsymbol{q}, \dot{\boldsymbol{q}})\dot{\boldsymbol{q}}$ is the vector of Coliolis and centrifugal forces, $\boldsymbol{f}_D$ is the vector consisting of the drag and lift forces. f_x and f_y are input forces of the X and Y directions, $\tau_i (i = 0, 1, 2)$ is the joint torque.

With respect to the base input $\boldsymbol{u}_B = [f_x \ f_y \ \tau_0]^T$ and joint input $\boldsymbol{u}_M = [\tau_1 \ \tau_2]^T$, matrices and vectors of Eq. 6 can be represented by the following block matrices:

$$\boldsymbol{M} = \begin{bmatrix} \boldsymbol{M}_{BB} & \boldsymbol{M}_{BM} \\ \boldsymbol{M}_{MB} & \boldsymbol{M}_{MM} \end{bmatrix}, \quad \boldsymbol{N} = \begin{bmatrix} \boldsymbol{N}_{BB} & \boldsymbol{N}_{BM} \\ \boldsymbol{N}_{MB} & \boldsymbol{N}_{MM} \end{bmatrix}$$

$$\boldsymbol{f}_D = \begin{bmatrix} \boldsymbol{f}_{DB}^T & \boldsymbol{f}_{DM}^T \end{bmatrix}^T, \quad \boldsymbol{u} = \begin{bmatrix} \boldsymbol{u}_B^T & \boldsymbol{u}_M^T \end{bmatrix}^T$$

Then, for a disturbance compensation described in the next section the following equation with respect to the base input can be obtained:

$$\boldsymbol{M}_{BB}\ddot{\boldsymbol{x}}_0 + \boldsymbol{M}_{BM}\ddot{\boldsymbol{\phi}} + \boldsymbol{N}_{BB}\dot{\boldsymbol{x}}_0 + \boldsymbol{N}_{BM}\dot{\boldsymbol{\phi}} + \boldsymbol{f}_{DB} = \boldsymbol{u}_B \tag{7}$$

3 Control method

3.1 Digital RAC[12]

Differentiating Eq. 1 with respect to time t, the following equation can be obtained:

$$\boldsymbol{W}(t)\boldsymbol{\alpha}(t) = \boldsymbol{\beta}(t) + \boldsymbol{f}(t) - \dot{\boldsymbol{W}}(t)\boldsymbol{v}(t) \tag{8}$$

where

$$\boldsymbol{W} = \begin{bmatrix} \boldsymbol{C} + \boldsymbol{E} & \boldsymbol{D} \\ \boldsymbol{A} & \boldsymbol{B} \end{bmatrix}, \quad \boldsymbol{\alpha} = \begin{bmatrix} \ddot{\boldsymbol{x}}_0^T & \ddot{\boldsymbol{\phi}}^T \end{bmatrix}^T$$

$$\boldsymbol{\beta} = \begin{bmatrix} \ddot{\boldsymbol{x}}_0^T & \ddot{\boldsymbol{p}}_e^T \end{bmatrix}^T, \quad \boldsymbol{f} = \begin{bmatrix} \dot{\boldsymbol{s}}^T & \boldsymbol{0}^T \end{bmatrix}^T, \quad \boldsymbol{v} = \begin{bmatrix} \dot{\boldsymbol{x}}_0^T & \dot{\boldsymbol{\phi}}^T \end{bmatrix}^T$$

and $\dot{\boldsymbol{s}}$ is the external force, including hydrodynamic force and thrust of the thruster, which act on the base.

Discretizing Eq. 8 by a sampling period T, and applying $\boldsymbol{\beta}$ and $\dot{\boldsymbol{W}}(k)$ to the backward Euler approximation, we have

$$\mathrm{W}(k)\boldsymbol{\alpha}(k-1)=\frac{1}{T}[\boldsymbol{\nu}(k)-\boldsymbol{\nu}(k-1)+T\boldsymbol{f}(k)- \{\boldsymbol{W}(k)-\boldsymbol{W}(k-1)\}\boldsymbol{\nu}(k)] \tag{9}$$

where $\boldsymbol{\nu}(k)=[\dot{\boldsymbol{x}}_0^T\ \dot{\boldsymbol{p}}_e^T]^T$. Note that a computational time delay is introduced into Eq. 9, and the discrete time kT is abbreviated to k.

For $\boldsymbol{\alpha}(k)$ and $\boldsymbol{\nu}(k)$ in Eq. 9, the desired acceleration $\boldsymbol{\alpha}_d(k)$ and velocity $\boldsymbol{\nu}_d(k)$ are defined as

$$\boldsymbol{\alpha}_d(k)=\frac{1}{T}\boldsymbol{W}^{-1}(k)[\boldsymbol{\nu}_d(k+1)-\boldsymbol{\nu}_d(k)+ \boldsymbol{\Lambda}\boldsymbol{e}_v(k)+T\boldsymbol{f}(k)] \tag{10}$$

$$\boldsymbol{\nu}_d(k)=\frac{1}{T}\{\boldsymbol{p}_d(k)-\boldsymbol{p}_d(k-1)+\boldsymbol{\Gamma}\boldsymbol{e}_p(k-1)\} \tag{11}$$

where $\boldsymbol{\Lambda}=\mathrm{diag}\{\lambda_i\}$ and $\boldsymbol{\Gamma}=\mathrm{diag}\{\gamma_i\}$ $(i=1,\ldots,5)$ are the velocity and position feedback gain matrices, $\boldsymbol{e}_v(k)=\boldsymbol{\nu}_d(k)-\boldsymbol{\nu}(k)$ and $\boldsymbol{e}_p(k)=\boldsymbol{p}_d(k)-\boldsymbol{p}(k)$ are the velocity and position error vectors, $\boldsymbol{p}_d(k)$ is the desired value of $\boldsymbol{p}(k)=[\boldsymbol{x}_0^T(k)\ \boldsymbol{p}_e^T(k)]^T$. When λ_i and γ_i are selected to satisfy $0<\lambda_i<1$ and $0<\gamma_i<1$, $\boldsymbol{e}_p(k)\to\boldsymbol{0}$ $(k\to\infty)$ is guaranteed.

In order to avoid the singular configuration of manipulator, the desired value of the base is modified by using the determinant of the Jacobian matrix $J(k)=\det\boldsymbol{J}(k)$ of manipulator. The desired linear acceleration of the base $\ddot{\boldsymbol{p}}_{0_d}=[\ddot{p}_{0x_d}\ \ddot{p}_{0y_d}]^T$ is defined as

$$\ddot{\boldsymbol{p}}_{0_d}=\begin{cases}\dot{\boldsymbol{p}}_{e_d} & (k_1\le k<k_1+n)\\ \boldsymbol{0} & (\text{otherwise})\\ -\dot{\boldsymbol{p}}_{e_d} & (k_2\le k<k_2+n)\end{cases}\ \backslash \tag{12}$$

where $\dot{\boldsymbol{p}}_{e_d}$ is the desired linear velocity of the end-tip of the manipulator, and k_1T and k_2T are the time when $|J(k)|$ becomes less or greater than a threshold J_s, respectively, and nT is the acceleration time.

3.2 Disturbance compensation

In general, added mass and moment of inertia and drag coefficient are used constant value that depends on the shape of robots.[13] Our proposed methods described above can reduce the influence of hydrodynamic force by position and velocity feedbacks.

Here, to obtain higher control performance, the influence of hydrodynamic force with respect to the base is treated as a disturbance and a disturbance compensation method is introduced.

The nominal model of $\boldsymbol{M}_{BB}$ in Eq. 7 is defined as $\bar{\boldsymbol{M}}_{BB}$. In $\bar{\boldsymbol{M}}_{BB}$ the added mass, added moment of inertia and the drag coefficient are constant. Furthermore, the following force is similarly defined:

$$\boldsymbol{f}_t=\bar{\boldsymbol{M}}_{BM}\ddot{\boldsymbol{\phi}}_d+\bar{\boldsymbol{N}}_{BB}\dot{\boldsymbol{x}}+\bar{\boldsymbol{N}}_{BM}\dot{\boldsymbol{\phi}}+\bar{\boldsymbol{f}}_{DB} \tag{13}$$

where $\bar{*}$ is nominal model of *.

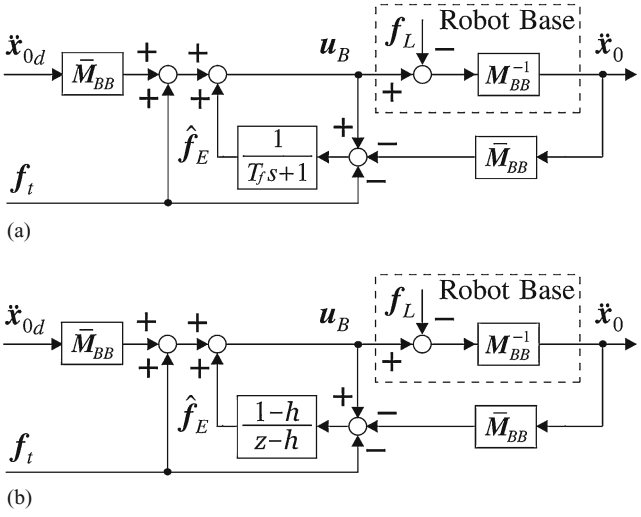

Fig. 3. Disturbance compensation. (**a**) analog version, (**b**) digital version

Table 1. Physical parameters of underwater robot

	Base	Link 1	Link 2
Mass [kg]	26.04	4.25	1.23
Moment of inertia [kg·m^2]	1.33	0.19	0.012
Link length (x) [m]	0.2	0.25	0.25
Link length (y) [m]	0.81	0.04	0.04
Link width [m]	0.42	0.12	0.12
Added mass (x) [kg]	72.7	1.31	0.1
Added mass (x) [kg]	6.28	3.57	2.83
Added moment of inertia [kg·m^2]	1.05	0.11	0.06
Drag coefficient (x)	1.2	0	0
Drag coefficient (y)	1.2	1.2	1.2

When the modeling error with respect to the hydrodynamic force regards the disturbance $\boldsymbol{f}_E$, the following estimated value can be obtained:

$$\hat{\boldsymbol{f}}_E=F(s)\left(\boldsymbol{u}_B-\bar{\boldsymbol{M}}_{BB}\ddot{\boldsymbol{x}}_{0_d}-\boldsymbol{f}_t\right) \tag{14}$$

where $F(s)=1/(T_fs+1)$ and $\ddot{\boldsymbol{x}}_{0_d}$ is the desired value of $\ddot{\boldsymbol{x}}_0$, T_f is a time constant.

Using Eqs. 13 and 14 we have the following control input of the base:

$$\boldsymbol{u}_B=\bar{\boldsymbol{M}}_{BB}\ddot{\boldsymbol{x}}_{0_d}+\boldsymbol{f}_t+\hat{\boldsymbol{f}}_E \tag{15}$$

The configuration of the disturbance compensation is shown in Fig. 3(a). In Fig. 3(a) $\boldsymbol{f}_L$ is the external force of the base excepting $\bar{\boldsymbol{M}}_{BB}\ddot{\boldsymbol{x}}_0$. Furthermore, for the digital control system Fig. 3(a) is discretized to Fig. 3(b),[15] and $h=e^{-T_f/T}$ in Fig. 3(b).

4 Experiment

In this section, to verify the effectiveness of the proposed control method, experiments are done.

Physical parameters of the underwater robot are shown in Table 1. The details of the system and the thruster characteristics are shown in the reference.[9]

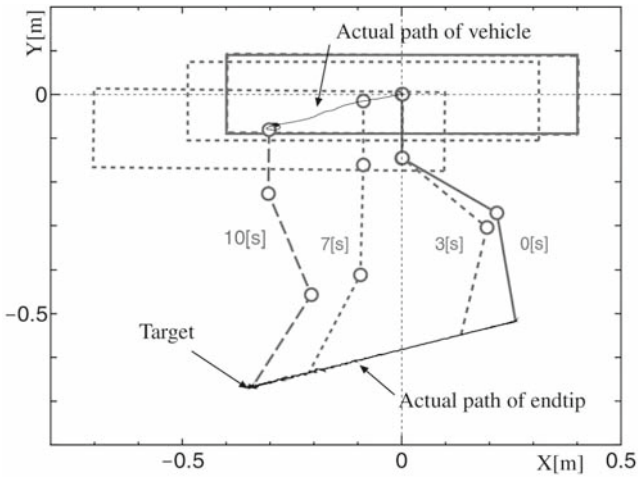

Fig. 4. Motion of the robot

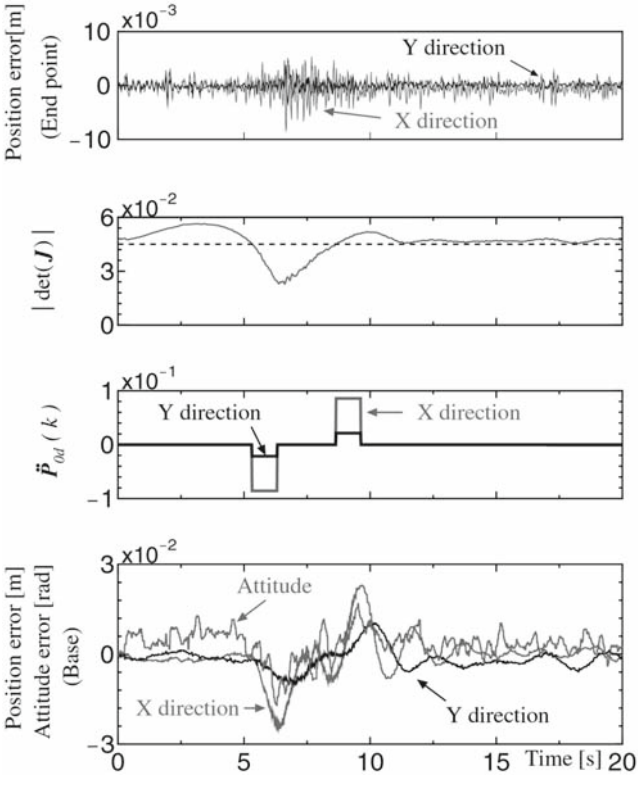

Fig. 5. Experimental result with disturbance compensation

The experiments are carried out under the following condition. The desired end-tip position is set up along a straight path from the initial position to the target. On the other hand, the basic desired position and attitude of the base is set up the initial values, and the threshold of the determinant of the Jacobian matrix is $J_s = 0.045$. The sampling period is $T = 1/60$ [s], the time constant of the filter is $T_f = 10$ [s], and the feedback gains are $\boldsymbol{\Lambda} = \mathrm{diag}\{0.3\ 0.3\ 0.2\ 0.2\ 0.2\}$ and $\boldsymbol{\Gamma} = \mathrm{diag}\{0.3\ 0.3\ 0.2\ 0.2\ 0.2\}$. Furthermore, the initial relative joint angles are $\phi_0 = -\pi/2$ [radΣ, $\phi_1 = \pi/3$ [rad] and $\phi_2 = -5\pi/18$ [rad].

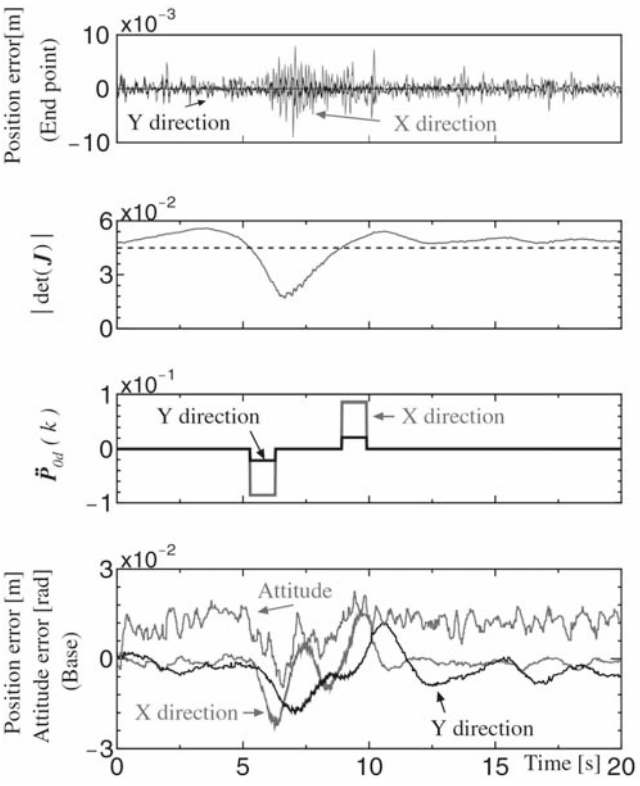

Fig. 6. Experimental result without disturbance compensation

The motion of the robot with the disturbance compensation is shown in Fig. 4. From Fig. 4, it can be seen that the end-tip follows the desired trajectory. The time histories of the results with and without the disturbance compensation are shown in Figs. 5 and 6, respectively. From these figures, we can see that the base position and attitude errors become small values using the disturbance compensation. Furthermore, reducing the base errors the end-tip position error is also reduced. Therefore, the control performance can be improved by using the proposed method.

5 Conclusion

In this paper, a digital RAC method for UVMS using disturbance compensation was proposed. The experimental results showed the effectiveness of the proposed method.

References

1. Maheshi H, Yuh J, Lakshmi R (1991) A coordinated control of an underwater vehicle and robotic manipulator. J Robotic Syst 8: 339–370
2. McLain TW, Rock SM, Lee MJ (1996) Experiments in the coordinated control of an underwater arm/vehicle system. Auton Robots 3:213–232
3. Tarn TJ, Shoults GA, Yang SP (1996) A dynamic model of an underwater vehicle with a robotic manipulator. Auton Robots 3:269–283

4. Antonelli G, Chiaverini S (1998) Task-priority redundancy resolution for underwater vehicle-manipulator systems. In: Proceedings of the 1998 IEEE ICRA, pp 768–773
5. Mclain TW, Rock SM (1998) Development and experimental validation of an underwater manipulator hydrodynamic model. Int J Robotics Res 17:748–759
6. Antonelli G, Caccavale F, Chiaverini S, et al (2000) Tracking control for underwater vehicle-manipulator systems with velocity estimation. IEEE J Oceanic Eng 25:399–413
7. Sarkar N, Podder TK (2001) Coordinated motion planning and control of autonomous underwater vehicle-manipulator systems subject to drag optimization. IEEE J Oceanic Eng 26:228–239
8. Antonelli G (2003) Underwater robots: motion and force control of vehicle-manipulator systems. Springer
9. Sagara S (2003) Digital control of an underwater robot with vertical planar 2-link manipulator. In: Proceedings of the 8th AROB, pp 524–527
10. Sagara S, Shibuya K, Tamura M (2004) Experiment of digital RAC for an underwater robot with vertical planar 2-link manipulator. In: Proceedings of the 9th AROB, pp 337–340
11. Yatoh T, Sagara S, Tamura M (2006) RAC for underwater vehicle-manipulator systems using dynamic equation. In: Proceedings of the 11th AROB, pp 233–236
12. Sagara S, Tamura M, Yatoh T, Shibuya K (2006) Digital RAC for underwater vehicle-manipulator systems considering singular configuration. Artif Life Robotics 10:106–111
13. Fossen TI (1995) Guidance and Control of Ocean Vehicles. John Wiley & Sons, pp 431–452
14. Levesque B, Richard MJ (1994) Dynamic analysis of a manipulator in a fluid environment. Int J Robot Res 13:221–231
15. Godler I, Honda H, Ohinishi K (2002) Design guidelines for disturbance observer's filter in discrete time. In: Proceedings of 7th International Workshop on Advanced Motion Control, pp 390–395